
VCD spectroscopy of chiral cinchona modifiers used in heterogeneous enantioselective hydrogenation: conformation and binding of non-chiral acids†

2 PERKIN

Thomas Bürgi,* Angelo Vargas and Alfons Baiker

Laboratory of Technical Chemistry, ETH Hönggerberg, HCI, CH-8093 Zürich, Switzerland

Received (in Cambridge, UK) 3rd April 2002, Accepted 18th June 2002

First published as an Advance Article on the web 10th July 2002

Vibrational circular dichroism (VCD) spectra of the chiral modifiers cinchonidine, an alkaloid, and (*R*)-2-(pyrrolidin-1-yl)-1-(1-naphthyl)ethanol (PNE) were measured and simulated. For cinchonidine independent information from NMR investigations on the distribution of conformers was used to simulate VCD spectra from calculated spectra of the individual conformers. Agreement with experiment is reasonably good. For the structurally similar synthetic modifier PNE VCD spectra show that an open conformer predominates in solution. The difference between the most stable conformers of cinchonidine and PNE in solution is the intramolecular hydrogen bond found in the latter, which forms due to the enhanced flexibility of the pyrrolidiny moiety in PNE as compared to the quinuclidine moiety in cinchonidine. The similar enantiodifferentiating power of cinchonidine and PNE as chiral modifiers in the heterogeneous enantioselective hydrogenation of ethyl pyruvate indicates that the rigidity of this part of the molecule is not a prerequisite for enantioselection. It is furthermore shown that binding of a non-chiral carboxylic acid to the alkaloid induces VCD in vibrations associated with the acid. Observation of this induced VCD allows probing of the chiral binding site.

Introduction

Modification of supported Pt metals by chiral molecules is a promising route for asymmetric catalysis using a heterogeneous process. One of the most studied reactions of this kind is the hydrogenation of C=O and C=C groups over modified Pt and Pd, respectively.^{1–4} It is believed that through adsorption of the modifier onto the metal the chiral information is brought to the active site.^{5,6} For the heterogeneous enantioselective hydrogenation of functionalized ketones over chirally modified Pt enantiomeric excesses of over 95% have been achieved. The best modifiers known up to now belong to the family of the cinchona alkaloids. The adsorption mode of the modifier, its conformation and its interaction with the reactant are key issues that need to be clarified in order to better understand the mechanism of enantiodifferentiation.

Vibrational circular dichroism (VCD) is the differential absorption of left- and right-circularly polarized infrared light by chiral molecules.^{7,8} Whereas enantiomers give identical infrared spectra, their VCD spectra have different signs. High sensitivity is required for VCD due to the small absorption differences. Besides being used for the determination of the absolute configuration of a molecule, VCD can also yield considerable information on its conformation.^{9,10} Here we demonstrate the potential of VCD spectroscopy for the study of (i) the conformation of modifiers in solution and (ii) their interaction with non-chiral carboxylic acids. We have previously studied in some detail the solvent-dependent conformational behavior of cinchonidine by NMR spectroscopy and *ab initio* calculations.¹¹ The findings from this study allow evaluation of the results from the VCD investigation. We now extend the conformational study to synthetic modifiers. Furthermore, we have studied complexes formed between cinchonidine and cinchonine, respectively, which are “pseudo-enantiomers”, and a

carboxylic acid, trifluoroacetic acid. The interaction between the modifiers and carboxylic acids is important for two reasons: (i) addition of carboxylic acids to the reaction mixture has a pronounced effect on enantioselectivity and acetic acid is in many cases the best solvent,¹² and (ii) alkenoic acids can be hydrogenated enantioselectively over cinchonidine-modified Pd.^{13–15} We will show that the chiral alkaloid induces VCD activity in the non-chiral acid that is bound to it.

The hydrogen-stretching region of quinidine, another member of the cinchona alkaloid family, has recently been studied by VCD spectroscopy.¹⁶ It was shown that this spectral region is useful for determining the absolute configuration and giving information on the conformation of the molecule. The study presented below is confined to the spectral region between 1700 and 1200 cm⁻¹.

Experimental and theoretical methods

VCD spectra were measured using a Bruker PMA 37 accessory coupled to an IFS/66 Fourier transform infrared spectrometer. The infrared beam from the spectrometer is polarized by a wire grid polarizer. The linearly polarized light is alternately switched at 50 kHz between left- and right-handed circular polarization by a photoelastic modulator (Hinds PEM 90) set at $\lambda/4$ retardation. The beam is transmitted through a cell equipped with CaF₂ windows and a Teflon spacer containing the chiral sample and is focused by a broadband-coated ZnSe lens onto a MCT detector. The detected signal is divided into two channels. The first signal, which contains the normal single beam spectrum, is low-pass filtered. The signal from the second channel contains the VCD spectrum and is high-pass filtered and demodulated at 50 kHz using a lock-in amplifier (SR830 DSP). Both signals are collected and stored simultaneously. An optical low-pass filter (<1800 cm⁻¹) was put before the photoelastic modulator. Before the actual sample was measured the phase was determined by measuring a VCD spectrum of a CdS multiple wavelength plate in combination with another polarizer. A single beam spectrum of the neat solvent served as

† Electronic supplementary information (ESI) available: Fig. S1, infrared spectra of the C–H and O–H stretching region of (*R*)-2-(pyrrolidin-1-yl)-1-(1-naphthyl)ethanol (PNE) in CCl₄. See <http://www.rsc.org/suppdata/p2/b2/b203251a/>

the reference for calculating the absorbance spectrum and a spectrum of the neat solvent recorded in VCD mode was subtracted from the VCD spectrum of the dissolved molecules. The data are presented without smoothing or further data processing. Performance of the system and applied procedures were tested by measuring samples of neat α -pinene. The results were in excellent agreement with reported spectra.¹⁷

Cinchonidine (Fluka purum), cinchonine (Fluka purum) and trifluoroacetic acid (Fluka puriss p.a.) were used as received. (*R*)-2-(Pyrrolidin-1-yl)-1-(1-naphthyl)ethanol (PNE) was synthesized as reported previously.¹⁸ To avoid significant contributions from self-association relatively low concentrations were used. As a consequence large path-lengths were needed in order to increase the signals and therefore not the entire spectrum of dissolved molecules is accessible due to strong solvent absorption.

All calculations were performed using the GAUSSIAN98 suite of programs.¹⁹ Complete optimization of all internal coordinates of the molecules was performed at the density functional B3LYP and B3PW91 levels of theory using a 6-31G* basis set. Several conformers were considered. For the minimized structures a normal coordinate analysis was performed. Rotational and dipole strengths associated with the normal modes were calculated in order to simulate absorption and VCD spectra using the equations:²⁰

$$\varepsilon(\tilde{\nu}) = \frac{8\pi^3 N}{3000hc(2.303)} \tilde{\nu} \sum_i D_i f_i(\tilde{\nu}, \tilde{\nu}_i)$$

$$\Delta\varepsilon(\tilde{\nu}) = \frac{32\pi^3 N}{3000hc(2.303)} \tilde{\nu} \sum_i R_i f_i(\tilde{\nu}, \tilde{\nu}_i)$$

Here D_i and R_i are the calculated dipole and rotational strengths and $\tilde{\nu}_i$ is the vibrational frequency.

$$f_i(\tilde{\nu}, \tilde{\nu}_i) = \frac{1}{\pi\gamma_i} \frac{\gamma_i^2}{[(\tilde{\nu} - \tilde{\nu}_i)^2 + \gamma_i^2]}$$

is the normalized Lorentzian line shape.

Results and discussion

Cinchonidine

Figs. 1 and 2 (bottom) show calculated infrared and VCD spectra, respectively, for three conformers of cinchonidine that were calculated to be the most stable. The structures of these conformers are shown in Fig. 3. The conformers differ in the relative orientation of the quinoline and quinuclidine moieties. At the B3LYP/6-31G* level Open(3) is calculated to be the most stable conformer followed by conformers Closed(1) and Closed(2), which are less stable by 1.6 and 2.3 kcal mol⁻¹. Other conformers are considerably higher up in energy. It has been shown earlier that when considering ΔG instead of ΔE , the conformers Closed(2) and Closed(1) become about equally stable.¹¹ The infrared spectra are not very sensitive towards conformation above about 1350 cm⁻¹, especially in the region of the quinoline vibrations above 1500 cm⁻¹. The calculated VCD spectrum for conformer Open(3) fits best with the observed spectrum. The largest discrepancy concerns the strong negative signal at just below 1300 cm⁻¹, observed in the experimental spectrum. This indicates the presence of closed conformers, which have stronger negative VCD signals at this position. The VCD signals of the quinoline vibrations are sensitive to the conformation, in contrast to the infrared spectrum. Comparison with Fig. 3 shows that the VCD pattern of the quinoline vibrations at 1510, 1570 and 1590 cm⁻¹ depends on the orientation of the quinoline moiety with respect to the O-H group. For the *trans* arrangement [Open(3) and Closed(2)] the

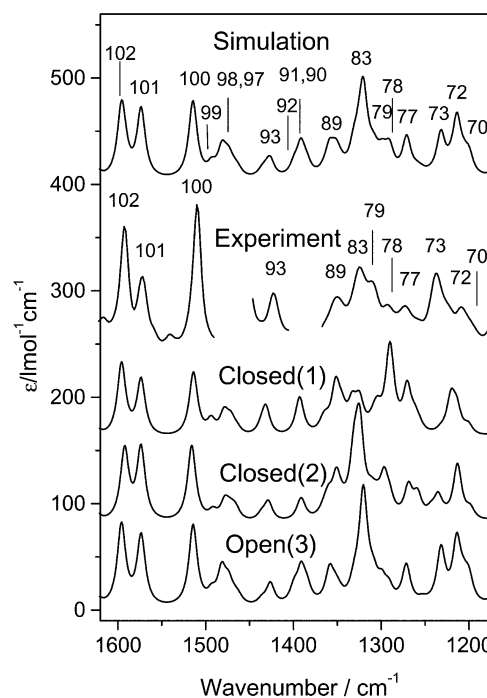


Fig. 1 Infrared spectra of cinchonidine. The spectra for conformers Open(3), Closed(1) and Closed(2) are derived from the dipole strengths calculated at the B3LYP level of theory using a 6-31G* basis set. Frequencies were scaled by 0.97. The spectra were simulated using a Lorentzian linewidth of 6 cm⁻¹. Experimental spectrum: 0.045 mol l⁻¹ solution of cinchonidine in CDCl₃, 1 mm path length, 6 cm⁻¹ resolution. Areas where strong solvent absorption interferes are omitted. The simulated spectrum (top trace) is composed of 70% Open(3), 15% Closed(1) and 15% Closed(2). The bands are labeled on the basis of a normal mode analysis of the most abundant conformer Open(3).

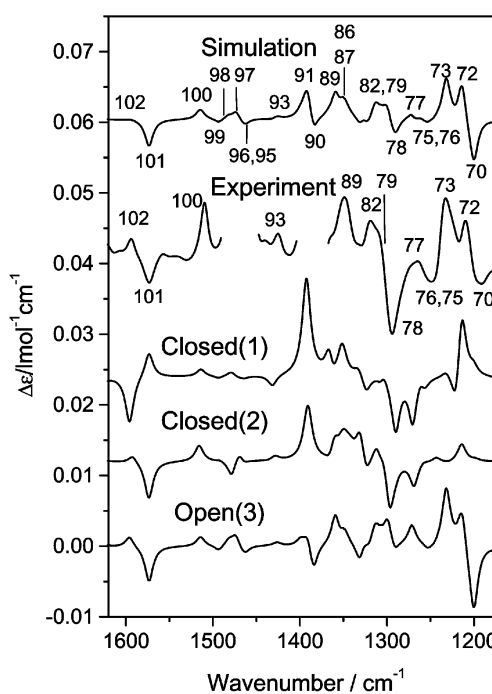


Fig. 2 VCD spectra of cinchonidine. The spectra for conformers Open(3), Closed(1) and Closed(2) are derived from the rotational strengths calculated at the B3LYP level of theory using a 6-31G* basis set. Frequencies were scaled by 0.97. The spectra were simulated using a Lorentzian linewidth of 6 cm⁻¹. Experimental spectrum: 0.045 mol l⁻¹ solution of cinchonidine in CDCl₃, 1 mm path length, 6 cm⁻¹ resolution. The spectrum was measured by averaging 3500 scans. Areas where strong solvent absorption interferes are omitted. The simulated spectrum (top trace) is composed of 70% Open(3), 15% Closed(1) and 15% Closed(2). The bands are labeled on the basis of a normal mode analysis of the most abundant conformer Open(3).

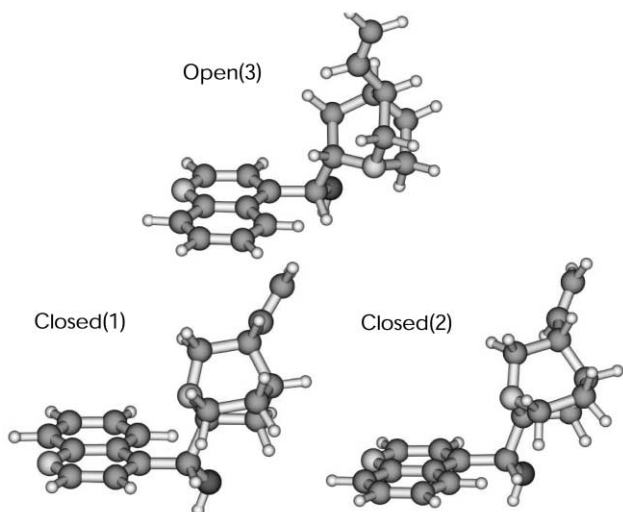


Fig. 3 Structure of the three most stable conformers of cinchonidine.

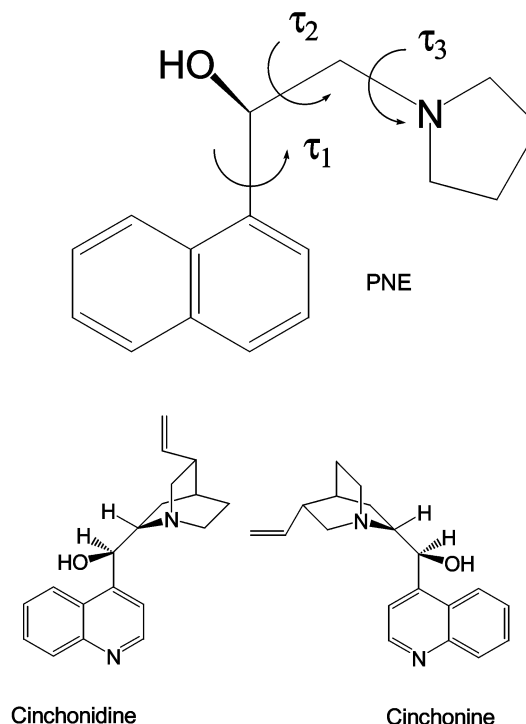
pattern is positive (1510 cm^{-1}), negative (1570 cm^{-1}), positive (1590 cm^{-1}), whereas for *cis* [Closed(1)] it is positive, positive, negative. Hence the measured spectrum clearly shows that the major conformer has a *trans* arrangement. This information is complementary to what has been found by NMR analysis, which was mainly sensitive to conformations being open or closed,¹¹ and agrees well with Open(3) being the most stable conformer.

From the investigation of the solvent-dependent conformational behavior of cinchonidine by NMR and *ab initio* calculations in combination with a reaction field model, it can be concluded that the fraction of conformer Open(3) in CDCl_3 (relative permittivity 4.8) is about 70%.¹¹ The residual 30% of the molecules adopt a closed conformation. From the calculation of ΔG and the fact that conformers Closed(1) and Closed(2) have similar dipole moments we can conclude that the stability of the two conformers is about the same in CDCl_3 . That is, from the information gained independently from VCD by calculations and NMR we may deduce a distribution of 70% Open(3), 15% Closed(1) and 15% Closed(2). Figs. 1 and 2 (top) also show a comparison between the experimental and simulated infrared and VCD spectra, respectively. For the simulations the following mixture of conformers was assumed: 70% Open(3), 15% Closed(1) and 15% Closed(2). In VCD, spectra of mixtures of conformers can be generated as a linear superposition of the spectra of the individual conformers. This is in contrast to NMR, where an averaged spectrum is usually measured, since the NMR experiment is slow compared to the inter-conversion between conformers. Both the simulated infrared and VCD spectra are in reasonably good agreement with experiment and hence the findings from NMR and VCD spectroscopy are consistent. The observed discrepancies between experiment and simulation can have several different origins. First of all, the distribution of conformers used for the simulation may not be completely correct. There are more important factors connected with the calculation of the dipole and rotational strengths, which may lead to discrepancies. Increase of the basis set is expected to yield more accurate values at the expense, however, of computer time. Also the treatment is based on the harmonic approximation and neglects solvent effects.

(*R*)-2-(Pyrrolidin-1-yl)-1-(1-naphthyl)ethanol

Molecules have been designed in the past that contain the essential parts for functioning as modifiers, which are an aromatic system, a stereogenic center and a N atom. One of these synthetic modifiers is (*R*)-2-(pyrrolidin-1-yl)-1-(1-naphthyl)ethanol (PNE).¹⁸ Compared to cinchonidine, PNE is more flexible

mainly due to the larger flexibility of the pyrrolidinyl compared to the quinuclidine part. The conformation of cinchonidine is largely determined by the relative arrangement of the quinoline and quinuclidine parts, which in turn is determined by two dihedral angles τ_1 and τ_2 (Scheme 1). In PNE one additional



Scheme 1 Top: structure of (*R*)-2-(pyrrolidin-1-yl)-1-(1-naphthyl)ethanol (PNE). τ_1 – τ_3 are the most important dihedral angles that determine the structure of the molecule. Bottom: structures of cinchonidine and cinchonine.

dihedral angle τ_3 is very flexible (Scheme 1). As a consequence of this enhanced flexibility the tertiary N is quite free to point in different directions for fixed τ_1 and τ_2 in PNE, whereas this is not true for cinchonidine. As a result of this flexibility PNE forms intramolecular hydrogen bonds, whereas cinchonidine does not. This effect shows itself as a characteristic broad band associated with the hydrogen bonded O–H at around 3450 cm^{-1} . An infrared spectrum of the O–H stretching region is provided in the electronic supplementary information (Fig. S1). For cinchonidine this band is missing.²¹ The very small band associated with free O–H at just above 3600 cm^{-1} shows that almost all the PNE is intramolecularly hydrogen-bonded. The fact that the O–H spectrum does not significantly change with concentration shows that the hydrogen bond is indeed intra- rather than inter-molecular.

This is in agreement with calculations, which show that the most stable conformers are hydrogen-bonded. The structures of the most stable conformers of PNE are shown in Fig. 4. Open(3)' is found to be most stable, followed by Open(4)' and Open(5)', which are less stable by 1.0 and 1.4 kcal mol⁻¹ at the B3PW91/6-31G* level. Corresponding energy differences of 1.1 and 2.4 kcal mol⁻¹ were found at the HF/6-31G* level. Other conformers are considerably higher up in energy by more than 3 kcal mol⁻¹, with the exception of Open(3) (Fig. 4), which is the analogue of the most stable conformer of cinchonidine. Conformers Open(3) and Open(3)' of PNE differ mainly in the dihedral angle τ_3 and the intramolecular hydrogen bonding, which is absent from Open(3). The latter is calculated to be less stable by about 2 kcal mol⁻¹ and therefore expected not to be populated significantly at room temperature.

Figs. 5 and 6 show the calculated infrared and VCD spectra for the three most stable conformers of PNE and the experimental spectra of solutions of PNE. The spectra of the

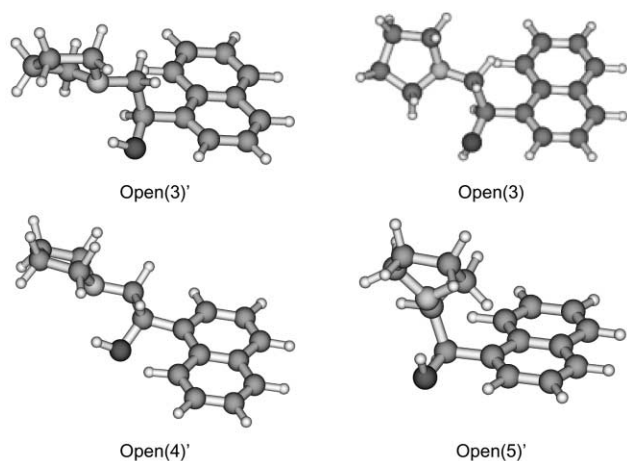


Fig. 4 Structures of the most stable conformers of PNE found by DFT calculations: Open(3)', Open(4)' and Open(5)', together with conformer Open(3). Open(3) and Open(3)' mainly differ in the dihedral angle τ_3 .

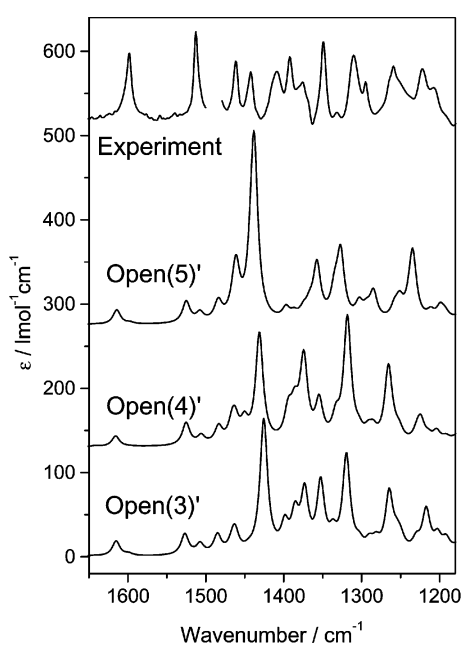


Fig. 5 Infrared spectra of PNE. The spectra for conformers Open(3)', Open(4)' and Open(5)' are simulated from the dipole strengths calculated at the B3PW91 level of theory using a 6-31G* basis set. Frequencies were scaled by 0.97. A Lorentzian linewidth of 6 cm^{-1} was used for the simulations. The experimental spectrum is composed from measurements in CCl_4 (from $1480\text{--}1345 \text{ cm}^{-1}$) and CDCl_3 (from $1650\text{--}1500$ and $1345\text{--}1180 \text{ cm}^{-1}$) solutions. Concentration: 0.022 mol l^{-1} (CCl_4) and 0.049 mol l^{-1} (CDCl_3), path lengths: 0.3 mm (CCl_4) and 0.2 mm (CDCl_3), resolution: 2 cm^{-1} . The experimental spectrum was scaled by a factor of two.

conformers differ considerably. The most prominent band in the calculated infrared spectra in the region shown in Fig. 5 is found at around 1425 cm^{-1} , which is associated with the O–H bending mode. Its position and intensity change considerably with conformation. In the calculated VCD spectra (Fig. 6) this band only shows up with large intensity for conformer Open(3)', for which this band is negative and the most prominent one in the frequency range shown. The measured spectrum exhibits this band, which is a strong indication that conformer Open(3)' prevails in solution. The corresponding infrared and VCD band at 1410 cm^{-1} is relatively broad, compared with the other bands in this frequency region, which is typical for a hydrogen bonded O–H group. Below 1400 cm^{-1} the calculated spectrum of conformer Open(3)' agrees best with the experimental one, although Open(4)' shows a quite similar

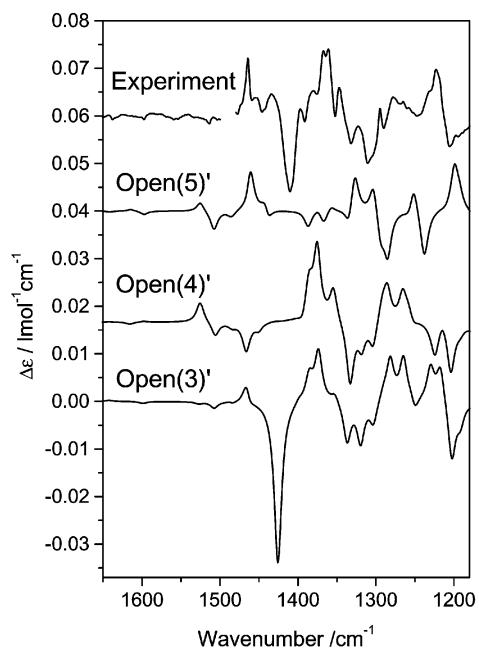


Fig. 6 VCD spectra of PNE. The spectra for conformers Open(3)', Open(4)' and Open(5)' are simulated from the rotational strengths calculated at the B3PW91 level of theory using a 6-31G* basis set. Frequencies were scaled by 0.97. A Lorentzian linewidth of 6 cm^{-1} was used for the simulations. The experimental spectrum is composed from measurements in CCl_4 (from $1480\text{--}1345 \text{ cm}^{-1}$) and CDCl_3 (from $1650\text{--}1500$ and $1345\text{--}1180 \text{ cm}^{-1}$) solutions. Concentration: 0.022 mol l^{-1} (CCl_4) and 0.049 mol l^{-1} (CDCl_3), path lengths: 0.3 mm (CCl_4) and 0.2 mm (CDCl_3), resolution: 2 cm^{-1} , average over 3500 scans.

pattern. Discrimination between conformers Open(3)' and Open(4)' can be made on the basis of the VCD signals above 1450 cm^{-1} . Whereas a positive signal is expected for conformer Open(3)' at around 1470 cm^{-1} , as observed, a negative signal is calculated for Open(4)'. Also the vibration associated with the naphthyl moiety at 1525 cm^{-1} shows only weak VCD activity for Open(3)', whereas a positive band is expected for Open(4)'. In the experimental spectrum no clear band can be discerned, which again shows that conformer Open(3)' predominates and that Open(4)' cannot be present in large amounts.

Cinchonidine–trifluoroacetic acid complex

Fig. 7 demonstrates the potential of VCD spectroscopy for probing complexes between chiral and non-chiral molecules. As an example the interaction between cinchonidine and the diastereomer (almost enantiomeric) cinchonine, respectively, and trifluoroacetic acid is studied. The interaction of the alkaloids with carboxylic acids is important in the field of heterogeneous enantioselective hydrogenation over modified platinum metals, where the alkaloid acts as the modifier that passes the chiral information to the metal catalyst and carboxylic acids are used as solvent, additives or substrates. It has been demonstrated earlier that carboxylic acids protonate the quinuclidine N of the alkaloid and that stable ion pair complexes are formed.^{21,22} It also became clear from infrared spectroscopy that the O–H group of the alkaloid is involved in the interaction.²¹ Fig. 7 (top) shows the proposed structure of a 1 : 1 acid–alkaloid complex. The figure also shows the infrared and VCD spectra of equimolar solutions of the alkaloids and trifluoroacetic acid. The dominant band in the spectra is associated with the antisymmetric carboxylate vibration, which is localized on the non-chiral molecule. Nevertheless, the spectra show that this mode exhibits VCD activity. Through its bonding to the chiral alkaloid VCD activity is induced in the non-chiral acid. Therefore the active vibration on the acid probes the chiral site to which it is bound. This is further corroborated by comparison

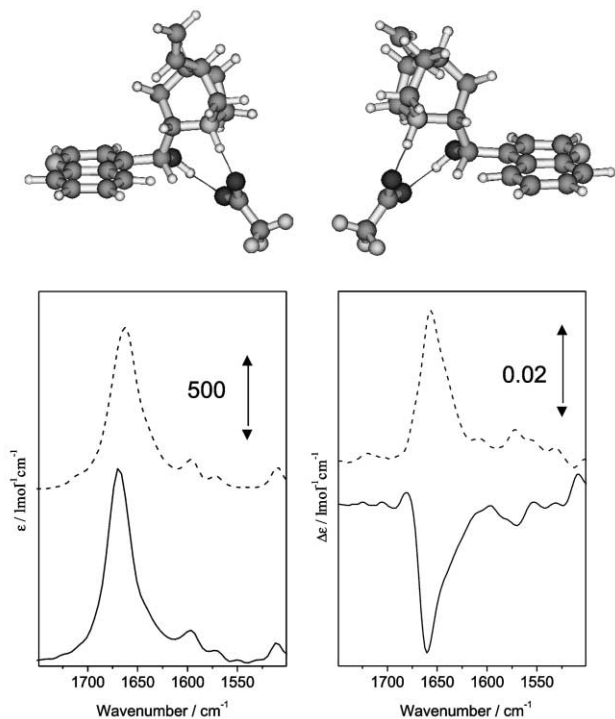


Fig. 7 Top: calculated structures of complexes between cinchonidine (left) and cinchonine (right), respectively, and trifluoroacetic acid. Lines represent hydrogen-bonding interactions. Bottom: infrared (left) and VCD spectra (right) of 1 : 1 mixtures (0.02 mol l^{-1}) of cinchonidine (solid line) and cinchonine (dashed line), respectively, and trifluoroacetic acid in CDCl_3 . Path length 0.2 mm , resolution 8 cm^{-1} , average of 3500 scans.

of the VCD spectra of acid bound to cinchonidine and cinchonine in Fig. 7. Although the two alkaloids are diastereomers (they differ in the position of the vinyl group, Scheme 1) the sites where the acid is bound to the two alkaloids are, to a good approximation, mirror images. As a consequence the carboxylate vibration is associated with a negative VCD signal in the case where the acid is bound to cinchonidine, whereas it shows a positive VCD signal for cinchonine. This also emerges from the calculations (B3LYP/6-31G*) which show rotational strengths for this vibration of $-460 \times 10^{-44} \text{ esu}^2 \text{ cm}^2$ for the complex with cinchonidine and $586 \times 10^{-44} \text{ esu}^2 \text{ cm}^2$ for the corresponding one with cinchonine. Typical rotational strengths of cinchonidine vibrations are smaller by about one order of magnitude.

The VCD signals strongly support the presence of the structures shown in Fig. 7 for the interaction complex between the alkaloids and the acid. Such a 1 : 1 interaction complex was proposed to play an important role in the enantioselective hydrogenation of alkenoic acids over cinchonidine-modified Pd.¹³ Alternatively, a cyclic 1 : 2 alkaloid–acid complex was suggested to be the crucial enantiodifferentiating entity.²³ The existence of the latter at high acid concentration was also indicated by infrared spectroscopy.²¹ For the enantioselective hydrogenation of carbonyl compounds over chirally modified Pt the quinuclidine N of the alkaloid, to which the trifluoroacetic acid is bound (Fig. 7), was proposed to interact with the reactant.³ Indeed, addition of a carboxylic acid to the reaction mixture can have significant effects on enantioselection. The relatively large stability of acid–base complexes between cinchonidine and carboxylic acids, as indicated by the VCD study, may indicate that the acid–base complex is the actual modifier that interacts with the reactant.²⁴

Conclusions

VCD spectroscopy is applied to investigate the solution conformation of modifiers used in the heterogeneous enantio-

selective hydrogenation over chirally modified Pt catalysts. For the alkaloid cinchonidine, the most used modifier, spectra were simulated from the calculated spectra of several conformers, whose abundance in solution is known independently from NMR and DFT calculations combined with reaction field models.¹¹ The NMR and VCD results agree well. For the synthetic modifier (*R*)-2-(pyrrolidin-1-yl)-1-(1-naphthyl)ethanol (PNE) an open conformer predominates in CDCl_3 and CCl_4 solutions. In contrast to cinchonidine, PNE forms intramolecular hydrogen bonds in solution, due to its larger flexibility compared to cinchonidine. For the heterogeneous enantioselective hydrogenation of ethyl pyruvate over modified Pt it has been shown that the quinuclidine N atom plays a fundamental role in enantiodifferentiation.²⁵ The VCD investigations demonstrate that in the most stable conformation of PNE and cinchonidine in solution the quinuclidine and pyrrolidinyl N, respectively, are quite differently oriented within the two molecules. Furthermore, for cinchonidine there is strong indication that the most stable conformer in solution, Open(3), is the one responsible for enantiodifferentiation.^{11,26} From the finding that both cinchonidine and PNE can efficiently induce enantioselection, one could conclude that the orientation of the N atom within the modifier is not crucial, which seems unlikely for a very selective reaction such as the one considered here. More likely to us seems the explanation that upon adsorption onto the Pt, which we have recently studied for cinchonidine,^{5,6} the intramolecular hydrogen bond in PNE is broken. Upon adsorption the aromatic moiety interacts with the metal surface and the dihedral angle τ_1 becomes fixed, whereas cinchonidine can still rotate around τ_2 and PNE around τ_2 and τ_3 . The enhanced flexibility of PNE around τ_3 may explain its slightly lower enantiodifferentiating power compared to cinchonidine. However, the example of PNE clearly demonstrates that rigidity in this degree of freedom is not crucial for enantiodifferentiation.

It is furthermore demonstrated by studying complexes between cinchonidine and cinchonine, respectively, and trifluoroacetic acid that VCD activity can be observed in the non-chiral part of the complex, *i.e.* in the acid. By measuring the VCD spectrum of the non-chiral molecule, the structure of the chiral binding site can be probed.

Acknowledgements

Grants of computer time by ETH-Zürich and CSCS in Manno are kindly acknowledged. Financial support was provided by ETH-Zürich and the Swiss National Science Foundation.

References

- 1 Y. Orito, S. Imai and S. Niwa, *J. Chem. Soc. Jpn.*, 1979, 1118.
- 2 H. U. Blaser, H. P. Jalett, M. Müller and M. Studer, *Catal. Today*, 1997, **37**, 441.
- 3 A. Baiker, *J. Mol. Catal. A: Chem.*, 1997, **115**, 473.
- 4 A. Baiker, *J. Mol. Catal. A: Chem.*, 2000, **163**, 205.
- 5 D. Ferri, T. Bürgi and A. Baiker, *Chem. Commun.*, 2001, 1172.
- 6 D. Ferri and T. Bürgi, *J. Am. Chem. Soc.*, 2001, **123**, 12074.
- 7 L. A. Nafie, T. A. Keiderling and P. J. Stephens, *J. Am. Chem. Soc.*, 1976, **98**, 2715.
- 8 L. A. Nafie, *Annu. Rev. Phys. Chem.*, 1997, **48**, 357.
- 9 A. Aamouche, F. J. Devlin and P. J. Stephens, *J. Am. Chem. Soc.*, 2000, **122**, 7358.
- 10 L. A. Nafie and T. B. Freedman, *Enantiomer*, 1998, **3**, 283.
- 11 T. Bürgi and A. Baiker, *J. Am. Chem. Soc.*, 1998, **120**, 12920.
- 12 H. U. Blaser, H. P. Jalett and J. Wiehl, *J. Mol. Catal.*, 1991, **68**, 215.
- 13 Y. Nitta and A. Shibata, *Chem. Lett.*, 1998, **161**, 161.

- 14 K. Borszeczy, T. Mallat and A. Baiker, *Catal. Lett.*, 1996, **41**, 199.
- 15 K. Borszeczy, T. Bürgi, Z. Zhaohui, T. Mallat and A. Baiker, *J. Catal.*, 1999, **187**, 160.
- 16 T. B. Freedman, F. Long, M. Citra and L. A. Nafie, *Enantiomer*, 1999, **4**, 103.
- 17 F. J. Devlin, P. J. Stephens, J. R. Cheeseman and M. J. Frisch, *J. Phys. Chem.*, 1997, **101**, 9912.
- 18 M. Schürch, T. Heinz, R. Aeschmann, T. Mallat, A. Pfaltz and A. Baiker, *J. Catal.*, 1998, **173**, 187.
- 19 M. J. Frisch, G. W. Trucks, H. B. Schlegel, G. E. Scuseria, M. A. Robb, J. R. Cheeseman, V. G. Zakrzewski, J. A. Montgomery, R. E. Stratmann, J. C. Burant, S. Dapprich, J. M. Millam, A. D. Daniels, K. N. Kudin, M. C. Strain, O. Farkas, J. Tomasi, V. Barone, M. Cossi, R. Cammi, B. Mennucci, C. Pomelli, C. Adamo, S. Clifford, J. Ochterski, G. A. Petersson, P. Y. Ayala, Q. Cui, K. Morokuma, D. K. Malick, A. D. Rabuck, K. Raghavachari, J. B. Foresman, J. Cioslowski, J. V. Ortiz, A. G. Baboul, B. B. Stefanov, G. Liu, A. Liashenko, P. Piskorz, I. Komaromi, R. Gomperts, R. L. Martin, D. J. Fox, T. Keith, M. A. Al-Laham, C. Y. Peng, A. Nanayakkara, C. Gonzalez, M. Challacombe, P. M. W. Gill, B. Johnson, W. Chen, M. W. Wong, J. L. Andres, M. Head-Gordon, E. S. Replogle and J. A. Pople, in *GAUSSIAN98*, Pittsburgh, PA, 1998.
- 20 J. A. Schellmann, *Chem. Rev.*, 1975, **75**, 323.
- 21 D. Ferri, T. Bürgi and A. Baiker, *J. Chem. Soc., Perkin Trans. 2*, 1999, 1305.
- 22 B. Minder, T. Mallat, P. Skrabal and A. Baiker, *Catal. Lett.*, 1994, **29**, 115.
- 23 K. Borszeczy, T. Mallat and A. Baiker, *Tetrahedron: Asymmetry*, 1997, **8**, 3745.
- 24 M. von Arx, T. Bürgi, T. Mallat and A. Baiker, *Chem. Eur. J.*, 2002, **8**, 1430.
- 25 H. U. Blaser, H. P. Jalett, D. M. Monti, A. Baiker and J. T. Wehrli, *Stud. Surf. Sci. Catal.*, 1991, **67**, 147.
- 26 M. Bartok, K. Felföldi, G. Szöllösi and T. Bartok, *Catal. Lett.*, 1999, **61**, 1.